Bi and Sr substitution effects on the spin-gap system Pb$_2$V$_3$O$_9$

Takeshi Waki,* Yutaka Itoh, Chishiro Michioka, and Kazuyoshi Yoshimura

Department of Chemistry, Graduate School of Science, Kyoto University, Kyoto 606-8502, Japan

Masaki Kato

Department of Molecular Science and Technology, Faculty of Engineering, Doshisya University, Kyo-Tanabe, Kyoto, Japan

We report the magnetic properties of Sr- and Bi-substituted samples of the one-dimensional alternating S =1/2 spin chain compound Pb$_2$V$_3$O$_9$. In the Sr-substituted system, we obtained two series of samples synthesized by different heat treatments; one series shows the reduction of the spin gap without antiferromagnetic long-range order (AF-LRO) and the other shows AF-LRO at low temperatures. We also observed impurity-induced AF-LRO in the Bi-substituted system. The fitting results of magnetic susceptibilities imply the possible coexistence of a spin gap and AF-LRO in both AF-LRO systems. These observations of AF-LRO with a small amount of substitution indicate that the magnetic instability involving a quantum critical point is inherent in the spin-gap system Pb$_2$V$_3$O$_9$.

I. INTRODUCTION

A quantum phase transition is one of the greatest topics in modern science. Spin-gap systems, such as spin-Peierls, spin alternation, dimer, two-leg ladder, and Haldane chain systems, do not undergo any magnetic long-range order even at zero temperature. The nonmagnetic ground state can be tuned by an external parameter such as the magnetic field or mechanical pressure, leading to an antiferromagnetic long-range ordered (AF-LRO) state. Recently, a field-induced AF-LRO in a spin-gap system was investigated intensively under the concept of the Bose-Einstein condensation (BEC) of *triplons*.[1–3]

It is known that a spin-gap ground state is tuned to the AF-LRO state also by chemical impurity substitution. The impurity-induced AF-LRO of spin-gap systems has been studied in several systems, such as (Cu$_{1-x}M_x$)GeO$_3$ (M=Zn,[4–8] Mn,[5] Ni,[5,8,9] Mg[10]), Sr(Cu$_{1-x}$Zn$_x$)$_2$O$_3$,[11] Pb(Ni$_{1-x}$Mg$_x$)$_2$V$_2$O$_8$,[12] Tl(Cu$_{1-x}$Mg$_x$)Cl$_3$,[13] Cu(Ge$_{1-x}$Si$_x$)O$_3$,[14] (CH$_3$)$_2$CHNH$_3$Cu(Cl$_{1-x}$Br$_x$)$_3$,[15,16] and Sr$_{14-x}$Ca$_x$Cu$_{24}$O$_{41}$.[17]

The substitution effects are classified into two categories: one is the substitution of magnetic sites by other magnetic or nonmagnetic ions, and the other is the substitution of nonmagnetic sites by other nonmagnetic ions. The former is usually called *site dilution* and the latter, *bond randomness*.

The site-dilution-type substitution generates unpaired spins at or near the substituted ions. Using a three-dimensional interaction, the unpaired spins order at low temperature. The coexistence of AF-LRO and a spin gap has been reported in several site-dilution-type substituted systems.[18,19]

On the other hand, bond-randomness-type substitution shows somehow different features. Cu(Ge$_{1-x}$Si$_x$)O$_3$ and (CH$_3$)$_2$CHNH$_3$Cu(Cl$_{1-x}$Br$_x$)$_3$ are a few examples of bond-randomness-type systems which undergo AF-LRO. The magnetic phase diagrams of both systems are quite different from each other. The Cu(Ge$_{1-x}$Si$_x$)O$_3$ system shows the co-existence of AF-LRO and a spin gap, while the (CH$_3$)$_2$CHNH$_3$Cu(Cl$_{1-x}$Br$_x$)$_3$ system shows AF-LRO exclusive of a spin-gap, indicating a quantum phase transition.

Quantum Monte Carlo simulations on a spin-gap system of the site-dilution and bond-dilution effects show interesting results. Site-dilution-type substitution induces AF-LRO with a small amount of impurity and shows the coexistence of a spin-gap and AF-LRO,[20] being consistent with several experimental results. On the other hand, the bond-dilution type, which can be regarded as an extreme example of bond-randomness system, undergoes a quantum phase transition from a spin-gapped to a gapless phase at finite impurity concentration.[21]

Recently, we have reported that the ground state of Pb$_2$V$_3$O$_9$ is of a gapped spin singlet and have also observed a field-induced AF-LRO with a low magnetic field.[22] The value of the spin gap is $\Delta/k_B \sim 7$ K, suggesting that this system is near a quantum critical point between the spin liquid and ordered phases. Therefore, this compound is possibly a new candidate for observing an impurity-induced AF-LRO by substituting on nonmagnetic sites. In this paper we report on the substitution effects on nonmagnetic Pb sites in Pb$_2$V$_3$O$_9$.

The crystal structure of Pb$_2$V$_3$O$_9$ is shown in Fig. 1. The compound has a triclinic structure (space group $C\bar{1}$). There are magnetic V^{4+}O$_6$ chains linking alternatively toward the [101] direction constructing one-dimensional (1D) S=1/2 alternating chains separated by nonmagnetic V^{5+}O$_4$ tetrahedrons and Pb ions.[23] As shown in Fig. 1, there are two crystallographically different Pb sites which are coordinated to seven and nine oxygen ions,[24] labeled as Pb(1) and Pb(2), respectively. Pb(1) and Pb(2) are located between two VO$_6$ chains and on one VO$_6$ chain, respectively.

As substituted ions for Pb sites, we choose Sr^{2+} and Bi^{3+} ions. By substituting Sr^{2+} for Pb^{2+}, we expect the bond-randomness effect because of the same valence and the different ion size. The (Pb$_{1-x}$Sr$_x$)$_2$V$_3$O$_9$ system is known to be synthesized by a solid-state reaction method in the whole Sr
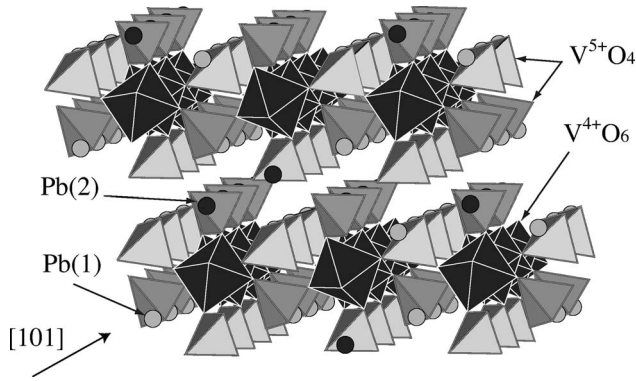
FIG. 1. Crystal structure of $Pb_2V_3O_9$. Two Pb sites are labeled as Pb(1) and Pb(2) indicated by light gray and dark gray spheres, respectively.

FIG. 2. Evolution of the lattice constants of Sr-substituted samples. Solid circles and open squares represent the data of 600 and 650 °C heat-treatment samples, respectively. The solid lines are guides for the eyes. The inset shows the unit-cell volume plotted against x.

content, $0 \leq x \leq 1$. At about $x = 0.25$, a structural transition from triclinic to monoclinic occurs[23] when x is increased. In the monoclinic phase, V^{4+} atoms make uniform chains, while in the triclinic phase they make alternating chains. For the purpose of studying the bond-randomness effect on the spin-gapped alternating chain, we investigate the triclinic phase with $x \leq 0.25$.

For Bi^{3+} substitution, we expect an electron-doping effect as well as a bond-randomness effect because the oxidization state of Bi is higher than that of Pb. The doped electron should lower the oxidization state of vanadium more than that in pure $Pb_2V_3O_9$. There are three kinds of vanadium ions in $Pb_2V_3O_9$ as shown in Fig. 1. Fourfold V ions must be V^{5+} judging from the ionic radius,[25] so that the doped electron should be on the sixfold V site: namely, an in-chain V^{4+}. That makes $V^{3+}(S=1)$ sites in places in the chain. Therefore, this substitution is regarded as the impurity effect of $S=1$ spin in an $S=1/2$ spin chain.

II. SAMPLES AND EXPERIMENTS

Polycrystalline samples of $(Pb_{1-x}Sr_x)_2V_3O_9$ $(x \leq 0.25)$ were prepared from mixtures of PbO, V_2O_3, V_2O_5, and $SrCO_3$ using standard solid-state reaction in sealed evacuated silica tubes. We synthesized two series of Sr-substituted samples. First, both samples were treated at 550 °C and made intermediate grindings several times; finally, we kept the samples at 600 °C (A) and 650 °C (B) for 2 days and then we cut off the furnace. Then, we successfully obtained two kinds of sample series with different magnetic properties that should be caused by a site preference of Sr ions for Pb sites. The details will be explained later. Hereafter, we call these systems Sr(A) and Sr(B).

$(Pb_{1-x}Bi_x)_2V_3O_9$ $(x \leq 0.040)$ samples were prepared from mixtures of PbO, V_2O_3, V_2O_5, and Bi_2O_3 by solid-state re-action in a sealed evacuated silica tube at 600 °C for 2 days after intermediate grindings. The Bi-substituted system of $Pb_2V_3O_9$ has not been reported so far. Bi-substituted samples have been synthesized in two final heat treatments at 600 and 650 °C. As neither x-ray diffraction (XRD) results nor mag-netic measurements of the two different heat-treatment
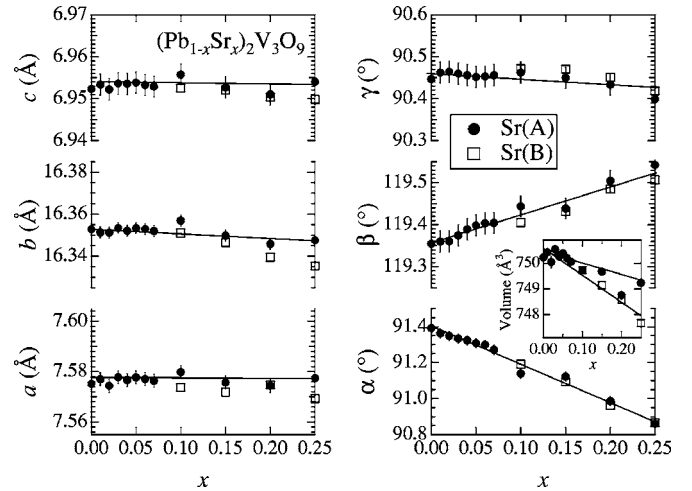
samples show different behaviors, we adopt the 600 °C samples hereafter.

The obtained samples were found to be in a single phase for Sr concentration $x \leq 0.25$ and for Bi concentration $x \leq 0.040$ by powder XRD measurements. To analyze the XRD patterns we use the RIETAN-2000 program.[26] However, it was difficult to determine the atomic positions and occu-pation ratios because of the low symmetry of the $Pb_2V_3O_9$ system and numerous atomic sites. Therefore, we only esti-mated the unit-cell parameters—i.e., the lattice constants a, b, c, α, β, and γ at room temperature. The temperature de-pendence of the magnetic susceptibility χ was measured down to 2 K at a magnetic field of 0.1 T using a supercon-ducting quantum interference devices (SQUID) magnetome-ter for three kinds of substituted systems: Sr(A), Sr(B), and Bi systems. Thermal analysis was performed using a differ-ential thermal analyzer (DTA) on a Sr-substituted sample in order to detect any structural change. Specific heat measure-ments were performed on a Bi-substituted sample by using a heat-relaxation method down to 2 K.

III. RESULTS

A. $(Pb_{1-x}Sr_x)_2V_3O_9$

Figure 2 shows the lattice parameters plotted against x for the Sr-substituted systems Sr(A) and Sr(B) exposed to 600 and 650 °C heat treatments. The x dependences of the lattice constants for two series of samples show similar behavior; the axis lengths a, b, and c are almost invariant or slightly decreasing and the angles α, β, and γ show continuous changes. The decrease of the unit-cell volumes for both Sr(A) and Sr(B) systems is observed, which is reasonable because the ionic radius of Sr^{2+} is smaller than that of Pb^{2+}.[27] The slight difference of unit-cell volumes between the Sr(A) and Sr(B) samples in the higher-Sr-concentration region sug-gests differences in the crystallographic structure.
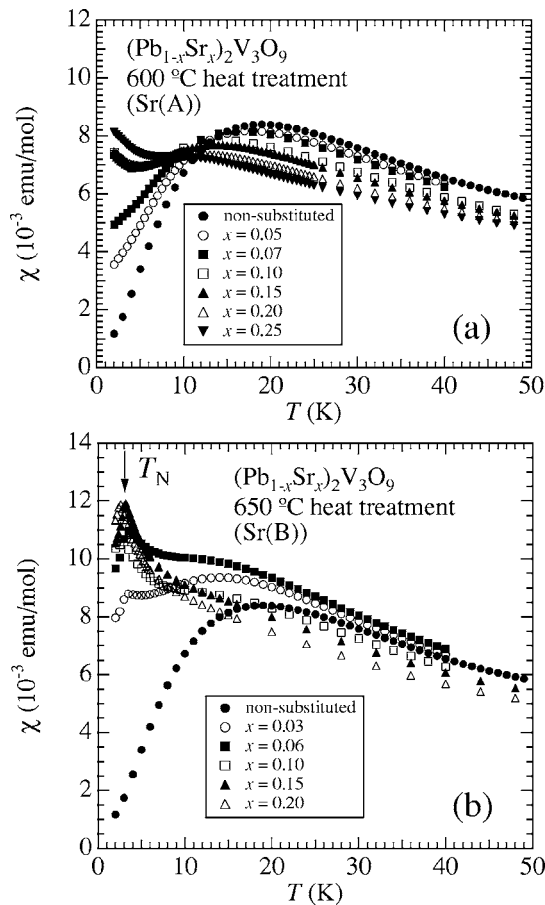
FIG. 3. Temperature and x dependences of χ of $(Pb_{1-x}Sr_x)_2V_3O_9$: (a) with 600 °C and (b) 650 °C heat treatments. Two types of Sr-substituted series show quite different magnetic properties. The peak magnitude and temperature of χ systematically decrease with increasing Sr content x in the Sr(A) series. In the Sr(B) series, with increasing x, the peak of χ at $T=20$ K indicating a low-dimensional feature faded and enhancement of Curie-Weiss-like behavior was observed.

The DTA measurement was done for a Sr-substituted sample, expecting some structural phase transition between 600 and 650 °C. Nevertheless, we have observed no anomalies between 600 and 650 °C, except anomalies at about 730 °C, indicating a melting point. This result obviously indicates that the difference between Sr(A) and Sr(B) is not because of the impurity phase generated by decomposition but is intrinsic. The difference may concern the site preference of Sr^{2+} ions discussed later.

Figure 3(a) shows the temperature dependence of χ of the Sr(A) samples with $0 \leq x \leq 0.25$. The temperature dependence of χ of the stoichiometric $Pb_2V_3O_9$ sample shows a maximum around $T=20$ K in agreement with 1D magnetic character. At the high-temperature region, it obeys the Curie-Weiss law. Below the temperature at which χ shows the maximum, χ decreases markedly. The whole shape is explained in terms of the $S=1/2$ alternating-spin-chain model. As x increases, both the broad maximum of χ and the temperature where χ takes the maximum gradually decrease, indicating suppression of the spin gap. The behavior of χ changes from that of an alternating spin chain to a Bonner-
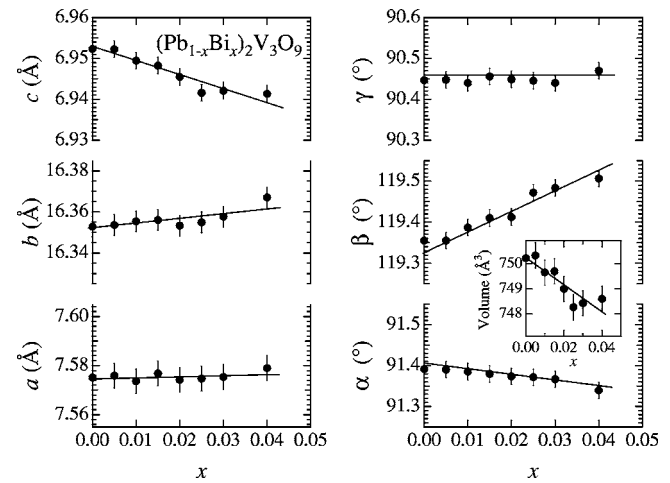
FIG. 4. Evolution of lattice constants as a function of x in $(Pb_{1-x}Bi_x)_2V_3O_9$. The solid lines are guides for the eyes. The inset shows the unit-cell volume plotted against x.

Fisher-type uniform spin chain as x increases. The low-temperature upturn, a Curie-Weiss term, is induced for $x > 0.10$. None of them, however, shows AF-LRO down to $T = 2$ K.

The temperature dependence of χ of the Sr(B) series is shown in Fig. 3(b). The behaviors of χ are quite different from those of the Sr(A) series samples. As x increases, the value of χ at $T=20$ K increases for $x \leq 0.06$, then decreases for $x \geq 0.10$. The broad maximum at about $T=20$ K is not suppressed for $x \leq 0.06$ but is rapidly suppressed for $x \geq 0.10$ and χ below $T=10$ K is enhanced. For $x \geq 0.06$, the upturn below $T=10$ K indicates a Curie-Weiss term due to unpaired moments. Above $x=0.10$, the maximum of χ at $T=20$ K disappears. At about $T=3$ K cusps of χ are observed even with a small amount of Sr substitution. The cusps indicate the appearance of AF-LRO, and we defined the temperature as T_N, which weakly depends on x as discussed later and shown in Fig. 7(b), below.

B. $(Pb_{1-x}Bi_x)_2V_3O_9$

In Fig. 4, we show the lattice constants as a function of Bi content x. One can find a systematic change of the lattice constants, which confirms a solid solution ranging as far as $x \leq 0.040$. The volume of the unit cell estimated from the lattice constants shrinks as Bi substitution proceeds. This is consistent with the fact that the Bi^{3+} ion is smaller than the Pb^{2+} ion.[27]

Figure 5 shows the temperature and x dependences of χ for Bi-substituted samples. As x increases, the magnitude of χ increases and the broad maximum around $T=20$ K is not suppressed but gradually masked by an additional Curie-Weiss term due to the doped electrons on vanadium ions by substituting Bi^{3+} for Pb^{2+}. The shape of the temperature dependence of χ can be understood by the superposition of alternating-chain behavior and Curie-Weiss behavior of the added moments.

The kinks of χ appear at about $T=3-6$ K for samples with $x \geq 0.010$. A specific-heat measurement for
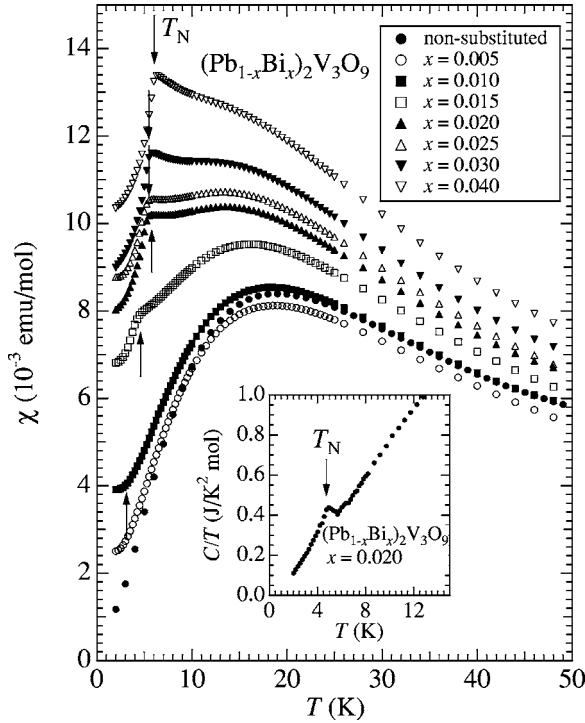
FIG. 5. Temperature and x dependences of χ of $(Pb_{1-x}Bi_x)_2V_3O_9$. As the Bi concentration x increases, the value of χ increases due to the doped electrons by Bi substitution. The arrows indicate the temperature where χ shows kinks, denoted by T_N. The inset is the temperature dependence of the specific heat divided by the temperature for $(Pb_{1-x}Bi_x)_2V_3O_9$ with $x=0.020$. The arrowed temperature denoted by T_N agrees with T_N determined by χ.

$(Pb_{1-x}Bi_x)_2V_3O_9$ with $x=0.020$ is shown in the inset of Fig. 5. An obvious peak of the specific heat divided by temperature, C/T, at 5 K indicates the magnetic phase transition with AF-LRO. The peak temperature of C/T agrees with the kink temperature of χ for $x=0.020$. Thus we regard the kink temperatures of χ as the Néel-ordering temperatures T_N, which depend on the Bi concentration x plotted later in Fig. 7(c).

As the substitution proceeds, electrons are doped into the $S=1/2$ alternating chain and are localized as $S=1$ impurity sites in places. Therefore, the increase of the value of χ should be explained by the increase of unpaired moments in the chain. The behavior of χ which can be explained by the superposition of the alternating-chain and Curie-Weiss models, suggests that the spin-gapped part and the extra unpaired moments coexist in the system.

IV. ANALYSIS

The temperature dependence of χ for pure $Pb_2V_3O_9$ is well described by an $S=1/2$ 1D alternating-Heisenberg-chain model.[3,23] In order to analyze the substitution effects on these substituted systems, we attempt to estimate the degree of the deviation of the substituted system from a pure one by fitting the temperature dependence of χ of substituted samples with the alternating-chain model.

The spin Hamiltonian for the 1D alternating Heisenberg chain is given by

$$H = -\sum_{i=1}^{N/2} (J_1 S_{2i-1} \cdot S_{2i} + J_2 S_{2i} \cdot S_{2i+1}), \qquad (1)$$

where N is the number of spins, J_1 the nearest-neighbor interaction, and J_2 the next-nearest-neighbor interaction. The alternation parameter is defined by $\alpha = J_2/J_1$. The numerical investigations suggest that the ground state of this model is a spin singlet when $0 \leq \alpha < 1$ for $S=1/2$.[28]

In Refs. 29 and 30, and the numerically calculated formula is proposed for χ in Eq. (1),

$$\chi_{alt}(T) = \frac{Ng^2\mu_B^2}{k_BT} \frac{A + By + Cy^2}{1 + Dy + Ey^2 + Fy^3}, \qquad (2)$$

where $y = |J_1|/2k_BT$, g is the g factor (now assuming as 2.0), μ_B is the Bohr magneton, and k_B is the Boltzmann constant. The numerical factors $A-F$ are the functions of α given in the references.

When substitution proceeds, the interaction of V^{4+}-V^{4+} (J_1 or J_2) near the substituted site should be changed. Actually, either J_1 or J_2 is rearranged by J_1' or J_2' randomly. It may be too simplified a picture that we apply Eq. (2) to substituted systems. However, it should give valuable information to estimate even an average value of the parameters.

As mentioned above, it seems that the temperature dependence of χ in the Sr(B)- and Bi-substituted systems is described by the superposition of alternating-chain and Curie-Weiss behavior. Then, for the analysis of these systems, we use the following function including a temperature-independent term and a Curie-Weiss term:

$$\chi(T) = \chi_{alt}(T) + \chi_0 + \frac{C}{T - \theta}, \qquad (3)$$

where χ_0, C, and θ are the temperature-independent term of χ, Curie constant, and Weiss temperature, respectively. Fittings are done in the temperature range of $8 \text{ K} \leq T \leq 300 \text{ K}$, because the numerical formula, Eq. (2), is applicable above $T = 0.25J_1/k_B$ (~ 8 K in this system).[29,30]

From the fitting results of the data in Figs. 3 and 5 with the function (3), we estimated J_1 and α for the substituted samples. We also estimate the spin-gap value Δ_{cal} using the following relation for a $S=1/2$ alternating-chain system as noted in Ref. 31:

$$\Delta_{cal} \simeq J_1 \left(1 - \frac{1}{2}\alpha - \frac{3}{8}\alpha^2 + \frac{1}{32}\alpha^3 + \cdots\right). \qquad (4)$$

The estimated $\Delta_{cal} \sim 15$ K from Eq. (4) for a pure sample is larger than the value ~ 7 K estimated from magnetization measurements. Although this suggests the importance of interchain interactions in this system, we focus only on the deviation of the substituted system from the pure one.

Figure 6 represents the typical fitting results of χ in each system. The fitting with Eq. (3) was available only in low degrees of substitution in each system. This is reasonable
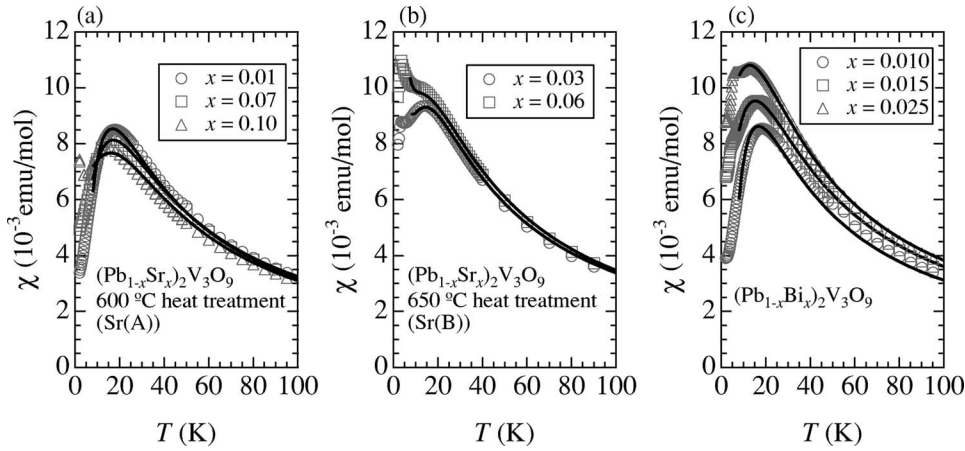
FIG. 6. The typical fitting curves of χ in (a) Sr(A), (b) Sr(B), and (c) Bi systems. Open marks show the raw data, and solid lines are fitting curves.

because the chains should be fragmented by substitution and finally deviate from the simple model described by Eq. (1) in the higher-concentration region.

Figure 6(a) shows the fitting results of the temperature dependence of χ of the Sr(A) system with Eq. (3) with $C=0$ for $0 \leqslant x \leqslant 0.10$. Over $x=0.10$, the temperature dependence of χ largely deviated from Eq. (3), even though χ still shows a low-dimensional feature.

The obtained values of the fitting parameters J_1 and α are plotted against x in the inset of Fig. 7(a). J_1 is almost invariant with the value of about 29 K against x, while α approaches 1.0. The evolution of α as a function of x indicates that the system approaches a uniform chain crystallographically or magnetically gapless phase.

When we assume that the magnitude of the exchange interaction depends only on the distance of the V^{4+}-V^{4+} bonding, the trend of J_1 and α as a function of x can be comprehended as below. In this alternating-chain model, J_1 corresponds to the interaction of a shorter-distance V^{4+}-V^{4+} couple and J_2 to a longer one. By substituting Pb for Sr, the average distance of V^{4+}-V^{4+} becomes shorter, because the size of Sr^{2+} is smaller than that of Pb^{2+}. The inset of Fig. 7(a) indicates that the shorter length corresponding to J_1 does not change, while α increases, suggesting an increase of J_2 or a shortening of the longer bonding. This is reasonable from the viewpoint of the ion size. The increase of β with x in the

XRD results also suggests that the average length of the longer bond corresponding to J_2 gradually becomes shorter.

We also estimated the value of Δ_{cal} by Eq. (4). The trend of the decrease of Δ_{cal} as a function of x with the gradient of $d\Delta_{cal}/dx=-140$ is clearly seen. The gradual decrease of Δ_{cal} by impurity substitution is consistent with the prediction for a bond-dilution system in Ref. 20 and for bond randomness in Ref. 32.

In Figs. 6(b) and 6(c), the fitting results of the Sr(B) and Bi substitution systems are shown, respectively. In low-concentration regions, the curves can be fitted by the superposition of a Curie-Weiss term and an alternating-chain model. The result implies the possibility of a spin gap and AF-LRO coexistence. For fitting χ in both systems, we fixed the value of J_1 as 29 K, on the analogy of the almost invariant J_1 for the Sr(A) system. Without this assumption, it was difficult to obtain meaningful fitting results with Eq. (3) because of a lot of variable parameters. From the fitting we obtained α, C, and θ. Using the obtained α and fixed $J_1=29$ K, we also estimate Δ_{cal} for the Sr(B) and Bi systems. In Figs. 7(b) and 7(c) we plot T_N and Δ_{cal} as a function of x for the Sr(B)- and Bi-substituted systems, respectively.

For the Sr(B)-substituted system, we also observed the decrease of Δ_{cal} as x decreases with the gradient of $d\Delta_{cal}/dx=-111$. The appearance of AF-LRO with a small amount of Sr substitution and also the possible coexistence
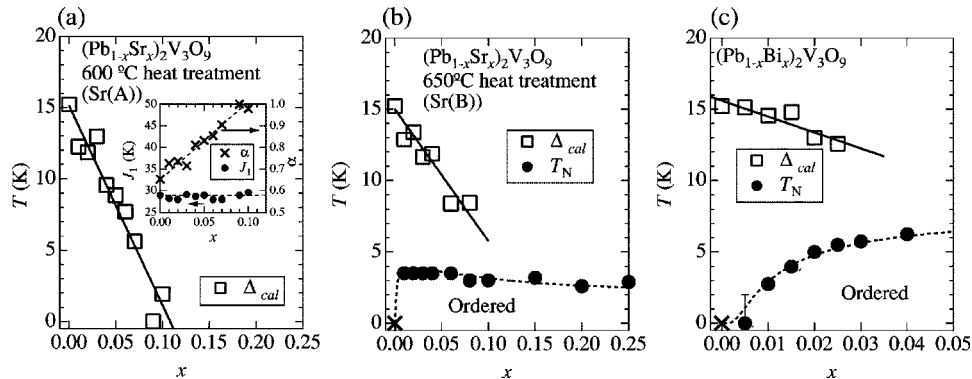
FIG. 7. T-x phase diagram of each substituted system: (a), (b), and (c) are for Sr(A)-, Sr(B)-, and Bi-substituted systems, respectively. Solid circles and open squares represent the Néel temperature T_N and spin gap Δ_{cal} in kelvin, respectively. Solid lines for Δ_{cal} values are fitting results by the least-squares method. Dashed lines are a guide for the eyes. The inset of (a) shows the evolution of the fitting parameter of J_1 and α as a function of x in $(Pb_{1-x}Sr_x)_2V_3O_9$.
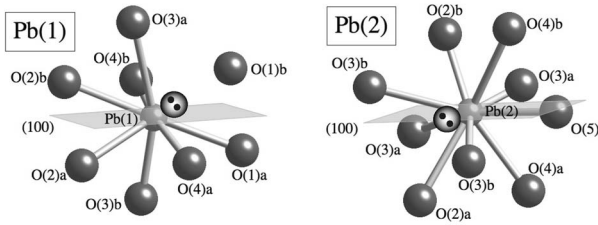
FIG. 8. Pb cations and $6s^2$ lone-pair environment. Pb(1) and Pb(2) are coordinated to seven and nine oxygen ions, respectively. The shaded planes show (100) planes. The labels of ions are named following Ref. 24. The distance between Pb(1) and O(1)b ions is longer than 3 Å, which is almost negligible as a chemical bond. The $6s^2$ lone pair is located at the open space between Pb(1) and O(1)b. The $6s^2$ lone pair on Pb(2) is directed to the open space within the Pb(2)-O(3)b-O(3)b-O(2)a-O(3)a pentahedra.

of a spin gap and AF-LRO have been observed. These behaviors are quite different from that of the Sr(A) system. Above $x=0.08$, the fitting was unsuccessful.

For the Bi-substituted system, the fit was done in the cases below $x=0.025$. We obtained α and Δ_{cal} as in the Sr(B) system. Above the concentration $x=0.025$, the fitting was unsuccessful. The obtained values of Δ_{cal} and T_N are plotted in Fig. 7(c). Δ_{cal} in the Bi system also decreases with increasing x with a gradient of $d\Delta_{cal}/dx=-92$.

As information of unpaired moments, we obtained the Curie constant as 0.0158 and 0.0432 emu K/mol for the Sr(B)-substituted sample with $x=0.06$ and Bi-substituted sample with $x=0.025$, respectively. We also obtained a θ value of about -5 K, indicating weak coupling of the unpaired moments.

Comparing the three phase diagrams for the Sr(A)-, Sr(B)-, and Bi-substituted systems, one can see several features as below.

(i) The decrease of Δ_{cal} with increasing x is observed in all three phase diagrams.

(ii) The gradient of $d\Delta_{cal}/dx$ of each system is estimated as -140, -111, and -92 for the Sr(A)-, Sr(B)-, and Bi-substituted systems, respectively.

(iii) AF-LRO is observed in the Sr(B)- and Bi-substituted systems.

V. DISCUSSION

A. Sr(A) vs Sr(B)

Although both Sr(A) and Sr(B) systems commonly show a decrease of Δ_{cal} with increasing x, the ground states of these systems are different; the Sr(A) system shows a spin-liquid state, the Sr(B) system an AF-LRO state. These two series were synthesized by differently controlled final treatment temperatures. Neither the structural phase transition nor phase separation was confirmed by DTA measurements between 600 and 650 °C. As one reason for the different magnetic properties of Sr(A) and Sr(B), we assume a change of the site preference of Sr ions under 600 and 650 °C heat treatments. There are two Pb sites with crystallographically
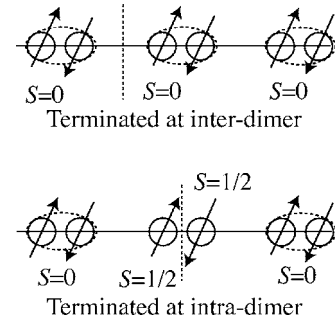
different circumstances: i.e., Pb(1) and Pb(2). Pb(1) connects the two vanadium spin chains, whereas Pb(2) connects one chain as shown in Fig. 1. It is not clear *a priori* whether Sr ions are equivalently substituted for the two Pb sites or not, when the substitution proceeds.

It is likely that Sr^{2+} is not substituted for the two Pb sites equivalently in the different heat treatments. That is, the difference between Sr^{2+} and Pb^{2+} is not only in size but in the existence of a lone pair. A Pb^{2+} ion has a $6s^2$ lone pair while the Sr^{2+} ion does not. This character with or without the lone pair possibly causes a site preference (see Fig. 8).

The structure of $Sr_2V_3O_9$, the another end side of the solid solution $(Pb_{1-x}Sr_x)_2V_3O_9$, is not isostructural but very close to that of $Pb_2V_3O_9$. $Sr_2V_3O_9$ has two Sr sites labeled Sr(1) and Sr(2) corresponding to Pb(1) and Pb(2). Sr(1) and Sr(2) are coordinated to eight and nine oxygen atoms, respectively.[23] The difference in the number of coordinated oxygen atoms between Pb(1) and Sr(1) is due to the $6s^2$ lone pair on the Pb^{2+} ion. From the crystallographic analysis, the position and direction of the lone pair have been determined in $Pb_2V_3O_9$.[24] Due to the $6s^2$ lone pair, Pb(1) can exist as seven-coordinated, so that it is, thermodynamically, not desirable for Sr^{2+} ions to be in a seven-coordinated site without a $6s^2$ lone pair.

The difference of the temperature of the heat treatments may introduce a change of the distribution ratio of Sr-ion substitution for Pb(1)/Pb(2) sites. The valence bond sums of Pb(1) and Pb(2) are 1.76 and 1.9, respectively,[24] supporting the conjecture that the more desirable site for the Sr^{2+} ion to substitute is the Pb(2) site. In that sense, in lower-temperature heat treatments, Sr tends to substitute only for the Pb(2) site. In higher-temperature heat treatments, Sr is able to be substituted for the Pb(1) site with a large enough activation energy. This discussion is also consistent with the fact that no difference in heat treatments was observed in the Bi substitution system. Because the Bi^{3+} ion also possesses the $6s^2$ lone pair, it shows no site preferences. Once Sr enters a Pb(1) site, the local structure near the substituted site becomes drastically distorted, leading a termination of the spin chain. That makes a fragment of finite chains in the systems.

In Fig. 9, schematic models of the termination of the spin chain for alternating chains are presented. The unpaired moments are possibly generated near the substituted ions by termination of the spin chain. Pb(1) sites link two magnetic

FIG. 9. Schematic model to explain how the impurity ion terminates the magnetic chain. There are two ways to terminate the spin chain: along interdimer and intradimer paths.

chains in $Pb_2V_3O_9$. These chains, located next to each other, have a different phase in the alternation of J_1 and J_2 so that the two edge moments are generated in either chain near the substituted Pb(1) site as shown Fig. 9. That leads to AF-LRO in the Sr(B) system without intensive electron doping.

The number of unpaired moments is calculated from the Curie constant for Sr(B) samples with $x=0.06$. Assuming $S=1/2$ free spin, 0.042/f.u. of unpaired spins are generated by substitution and are smaller than the 0.12/f.u. estimated based on the case that all substituted Sr ions enter the Pb(1) site and cut the chain making unpaired moments as in Fig. 9(b). Conversely, we may estimate the degree of Pb(1) site occupation of the Sr ion based on the above view: 0.042/f.u. $S=1/2$ spins for $x=0.06$ corresponds to the case that 35% of the substituted ions are in Pb(1) sites.

For simplicity, one may assume that Pb(1) substitution acts only as termination of the spin chains without any change in interaction, whereas Pb(2) substitution causes weak modulation in the interaction. This hypothesis can explain why the absolute value of $d\Delta_{cal}/dx$ of Sr(A) is larger than that of Sr(B). The ratio of the slants, $d\Delta_{cal}/dx$, for Sr(B) and Sr(A) is $-111/-140=0.8$, giving relatively good agreement with the estimation from the Curie constant. In a word, almost all the doped Sr^{2+} ions are substituted for the Pb(2) site in the Sr(A) system, while the Sr^{2+} ions are partially substituted for Pb(1) and Pb(2) in the Sr(B) system.

The impurity-induced AF-LRO with bond-randomness-type substitution has been observed only in $Cu(Ge_{1-x}Si_x)O_3$ and $(CH_3)_2CHNH_3Cu(Cl_{1-x}Br_x)_3$. This Sr(B) series is a new example of bond-randomness-type AF-LRO.

B. Sr(B) vs Bi

In both the Sr(B)- and Bi-substituted systems, there is the possibility of the coexistence of a spin gap and AF-LRO in the small-x region. Judging from the increase of magnitude of χ as the substitution proceeds, unpaired moments are induced in both systems [Sr(B), $x\leq0.06$]. However, the origin of the unpaired moments in the Bi system seems to be different from that in the Sr(B) system. In the Sr(B) system, as mentioned above, they are possibly generated by cutting the spin dimers.

In a site-dilution-type system, unpaired moments are generated by the substitution of magnetic ions. That is, in an $S=1/2$ spin system, the ions are changed by other ones with $S=0$ or $S=1$, etc. That situation prevents ions from making dimer pairs, resulting in the appearance of unpaired moments. The Haldane-gap system is a little bit different but we discuss it based on the dimer-based system.

In the Bi-substituted system, the unpaired moments should be due to the doped electrons. As mentioned above, the electron should be doped on the sixfold vanadium ion because of crystallographic reasons.

The small number of unpaired moments estimated from the Curie constant excludes a simple idea that a doped electron acts as a free moment on dimers. The Curie constant for the Bi system with $x=0.025$ is 0.0432 emu K/mol. Assuming an $S=1/2$ moment, the number of moments is calculated as 0.115/f.u. from the Curie constant, which is about twice

as many as that of the doped electrons, 0.05/f.u., calculated from the chemical composition. It is even more reasonable to consider that the $S=1$ spins on V^{3+} sites are screened by spins around them, rather than that the added spins act as unpaired $S=1/2$ spins on singlet dimers, because the Curie constant from $S=1$ spins is estimated as 0.05 emu K/mol for the $x=0.025$ sample.

From our experiment, it is unclear whether the doped electron is completely localized at one vanadium ion or hopping between bound states even though it seems that the electron is near the substituted Bi^{3+} ion for electrostatic reasons.

The ordered moments below T_N should be the generated unpaired moments in both systems. However, the evolutions of T_N as a function of x are quite different from each other. In the Bi-substituted system, T_N increases with x increasing, showing a "dome"-like shape. This type of T_N dependence is seen in several site-dilution AF-LRO systems. On the other hand, in the Sr(B)-substituted system, T_N is almost invariant against or weakly dependent on x. The difference between these two impurity effects on T_N may be caused by the type of generation of unpaired moments. We need further information to discuss this problem in detail.

The phase diagram of the Bi-substituted system which shows a reduction of Δ_{cal} and possible coexistence of a spin gap and AF-LRO is quite similar to those of the other site-dilution systems: e.g., $(Cu_{1-x}M_x)GeO_3$, $M=Zn^{2+}(S=0)$ or $Ni^{2+}(S=1)$. Since no direct substitution for V^{4+} but the indirect substitution effect on V^{4+} is observed, our $(Pb_{1-x}Bi_x)_2V_3O_9$ system is a new type of impurity-induced magnetic ordering by changing the valence state of magnetic sites as in the $Sr_{14-x}Ca_xCu_{24}O_{41}$ system.[17]

VI. SUMMARY

We have studied the substitution effects of the nonmagnetic Pb site on the spin-gap system $Pb_2V_3O_9$. We observed an impurity-induced AF-LRO by substituting Sr(B) (with 650 °C heat treatment) and Bi for Pb site. For the Sr(B)-substituted system, AF-LRO is induced by bond-randomness effects. In the Bi-substituted system, the enhancement of unpaired moments with a small amount of substitution results in Néel order, similarly to the case of other site-dilution-type systems. To our knowledge this type of impurity-induced AF-LRO by doped electrons due to nonmagnetic ion substitution with different valence is seldom reported. The successful fitting results of the spin susceptibility suggests that the substituted systems keep the alternating-chain features. Judging from these results and a small amount of ordered moment estimated from the specific-heat result, most of spins are inactive at low temperatures, implying the possible coexistence of Néel order and a spin gap in Sr(B) and Bi systems. In the Sr(A) doping system with 600 °C heat treatment, reduction of the spin gap was observed. No AF-LRO was observed down to $T=2$ K, just in a gapless phase. Although the quantum phase transition behavior which is a coincidence of the disappearance of the spin gap and the appearance of AF-LRO has not been confirmed in this experiment, a quantum critical point might be realized in Sr(A)-substitution systems.

ACKNOWLEDGMENTS

*Electronic address: twac@kuchem.kyoto-u.ac.jp

[1] T. Nikuni, M. Oshikawa, A. Oosawa, and H. Tanaka, Phys. Rev. Lett. **84**, 5868 (2000).

[2] M. Jaime, V. F. Correa, N. Harrison, C. D. Batista, N. Kawashima, Y. Kazuma, G. A. Jorge, R. Stein, I. Heinmaa, S. A. Zvyagin, Y. Sasago, and K. Uchinokura, Phys. Rev. Lett. **93**, 087203 (2004).

[3] T. Waki, Y. Morimoto, C. Michioka, M. Kato, H. Kageyama, K. Yoshimura, S. Nakatsuji, O. Sakai, Y. Maeno, H. Mitamura, and T. Goto, J. Phys. Soc. Jpn. **73**, 3435 (2004).

[4] M. Hase, I. Terasaki, Y. Sasago, K. Uchinokura, and H. Obara, Phys. Rev. Lett. **71**, 4059 (1993).

[5] S. B. Oseroff, S. W. Cheong, B. Aktas, M. F. Hundley, Z. Fisk, and L. W. Rupp, Jr., Phys. Rev. Lett. **74**, 1450 (1995).

[6] M. Hase, N. Koide, K. Manabe, Y. Sasago, K. Uchinokura, and A. Sawa, Physica B **215**, 164 (1995).

[7] M. Hase, K. Uchinokura, R. J. Birgeneau, K. Hirota, and G. Shirane, J. Phys. Soc. Jpn. **65**, 1392 (1996).

[8] J.-G. Lussier, S. M. Coad, D. F. McMorrow, and D. McK Paul, J. Phys.: Condens. Matter **7**, L325 (1995).

[9] N. Koide, Y. Sasago, T. Masuda, and K. Uchinokura, Czech. J. Phys. **46**, 1981 (1996).

[10] T. Masuda, I. Tsukada, K. Uchinokura, Y. J. Wang, V. Kiryukhin, and R. J. Birgeneau, Phys. Rev. B **61**, 4103 (2000).

[11] M. Azuma, Y. Fujishiro, M. Takano, M. Nohara, and H. Takagi, Phys. Rev. B **55**, R8658 (1997).

[12] Y. Uchiyama, Y. Sasago, I. Tsukada, K. Uchinokura, A. Zheludev, T. Hayashi, N. Miura, and P. Boni, Phys. Rev. Lett. **83**, 632 (1999).

[13] A. Oosawa, T. Ono, and H. Tanaka, Phys. Rev. B **66**, 020405(R) (2002).

[14] L. P. Regnault, J. P. Renard, G. Dhalenne, and A. Revcolevschi, Europhys. Lett. **32**, 579 (1995).

[15] H. Manaka, I. Yamada, H. Mitamura, and T. Goto, Phys. Rev. B **66**, 064402 (2002).

[16] H. Manaka, I. Yamada, and H. Aruga Katori, Phys. Rev. B **63**, 104408 (2001).

[17] T. Nagata, H. Fujino, K. Satoh, N. Yamamori, J. Akimitsu, S. Katano, M. Nishi, K. Kakurai, M. Hiroi, M. Sera, N. Kobayashi, K. Tenya, H. Amitsuka, T. Takigawa, H. Inago, and T. Sakakibara, J. Phys. Soc. Jpn. **70**, 2419 (2001).

[18] A. Oosawa, M. Fujisawa, K. Kakurai, and H. Tanaka, Phys. Rev. B **67**, 184424 (2003).

[19] M. Azuma, M. Takano, and R. S. Eccleston, J. Phys. Soc. Jpn. **67**, 740 (1998).

[20] C. Yasuda, S. Todo, M. Matsumoto, and H. Takayama, Phys. Rev. B **64**, 092405 (2001).

[21] C. Yasuda, S. Todo, M. Matsumoto, and H. Takayama, Prog. Theor. Phys. Suppl. **145**, 339 (2002).

[22] T. Waki, Y. Morimoto, M. Kato, K. Yoshimura, H. Mitamura, and T. Goto, Physica B **359-361**, 1372 (2005).

[23] O. Mentre, A. C. Dhaussy, F. Abraham, and H. Steinfink, J. Solid State Chem. **140**, 417 (1998).

[24] O. Mentre, A. C. Dhaussy, F. Abraham, E. Suard, and H. Steinfink, Chem. Mater. **11**, 2408 (1999).

[25] S. Boudin, A. Guesdon, A. Leclaire, and M. M. Borel, Int. J. Inorg. Mater. **2**, 561 (2000).

[26] F. Izumi and T. Ikeda, Mater. Sci. Forum **321-324**, 198 (2000).

[27] R. D. Shannon, Acta Crystallogr., Sect. A: Cryst. Phys., Diffr., Theor. Gen. Crystallogr. **32**, 751 (1976).

[28] J. C. Bonner and M. E. Fisher, Phys. Rev. **135**, A640 (1964).

[29] J. W. Hall, W. E. Marsh, R. R. Weller, and W. E. Hatfield, Inorg. Chem. **20**, 1033 (1981).

[30] W. E. Hatfield, J. Appl. Phys. **52**, 1985 (1981).

[31] T. Barnes, J. Riera, and D. A. Tennant, Phys. Rev. B **59**, 11384 (1999).

[32] S. Todo (private communication).